National Conference with International Participation

ENGINEERING MECHANICS 2008

Svratka, Czech Republic, May 12 – 15, 2008

SIMPLE NUMERICAL MODEL OF LAMINATED GLASS BEAMS

A. Zemanová*, J. Zeman**

Summary: *The present contribution presents a simple Finite Element model aimed at an efficient formulation of layered glass units. The adopted approach is based on considering independent kinematics of each layer, tyied together via Lagrange multipliers. Validation and verification of the resulting model against idenpendent data demonstrates the model accuracy, showing its potential for generalization towards more complex problems.*

1 Introduction

Laminated glass is a multilayer material produced by bonding two or more layers of glass together with a plastic interlayer, typically made of polyvinyl butyral (PVB). The interlayer keeps the layers of glass bonded even when broken, and its high strength prevents the glass from breaking up into large sharp pieces. This produces a characteristic ”spider web” cracking pattern when the impact is not powerful enough to completely pierce the glass. Multiple laminae and thicker glass increase the strength of a structural member, too.

The most frequent approach to the analysis of glass structural elements was, for a long time, based on empirical knowledge. Such relations are sufficient for the design of traditional windows glasses. In modern architecture there has been a steadily growing demand on the use of transparent materials for large external walls and roof systems in the recent decades. Therefore, the detailed analysis of layered glass units is becoming increasingly important in order to ensure a reliable and efficient design.

2 Methods

In general, the complex behavior of laminated glass can be considered as an intermediate state of two limiting cases (Vallabhan et al., 1987). In the first case, the structure is treated as an assembly of two independent glass plates without any interlayer (the lower bound on stiffness and strength of a member), while in the second case, corresponding to the upper estimate of strength and stiffness, the glass unit is modeled as a monolithic glass (one glass plate with thickness equal to the total thickness of the glass plates). Both elementary cases, however, fail to correctly capture complex interaction among individual layers, leading to non-optimal layer thickness designs. Therefore, several alternative approaches to analysis of layered glass structures were proposed in the literature. These methods can be categorized into three basic groups:

- methods calibrated with respect to experimental measurements (Norville et al., 1998),

*Ing. Alena Zemanová: Department of Mechanics, Faculty of Civil Engineering, Czech Technical University in Prague, Thákurova 7, 166 29 Prague 6; tel.: +420 224 354 472; e-mail: zemanova.alena@gmail.com

**Ing. Jan Zeman, Ph.D.: Department of Mechanics, Faculty of Civil Engineering, Czech Technical University in Prague, Thákurova 7, 166 29 Prague 6; tel.: +420 224 354 482; e-mail: zemanj@cml.fsv.cvut

- analytical approaches (Vallabhan et al., 1993; Asik, 2003; Asik and Tezcan, 2005),
- numerical models typically based on detailed Finite Element simulations (Duser et al., 1999; Ivanov, 2006).

Applicability of analytical approaches to practical (usually large-scale) structures is far from being straightforward. In particular, the closed-form solution of the resulting equations is possible only for very specific boundary conditions and therefore usually have to be solved by an appropriate numerical method anyway. Moreover, they are difficult to be generalized to analysis of beams with multiple layers. Therefore, it appears to be advantageous to directly formulate the problem in the discretized form, typically based on the Finite Element Method (FEM). Nevertheless, the detailed numerical modeling of the complete structure based on two-dimensional (Ivanov, 2006) or even three-dimensional finite elements (Duser et al., 1999) leads to unnecessary expensive calculations.

In this paper, we propose a simple FEM model inspired by a specific class of refined plate theories (Mau, 1973; Šejnoha, 1996; Matouš et al., 1998). In this framework, each layer of the model is treated as a Timoshenko beam with independent kinematics. Interaction between individual layers is captured by the Lagrange multipliers (with a physical meaning of shear stresses), which result from the conditions of inter-layer displacements compatibility. Such a refined approach circumvents the limitation of similar models available in typical commercial FEM systems, which use a single set of kinematic vvariables and average the mechanical response through the thickness of the beam, e.g. (Bathe, 1996). Unlike the proposed numerical model, the averaging operation is still too simple to correctly represent the inter-layer interactions, see Section 5 for a concrete example.

3 Mechanical model of laminated beam

As illustrated by Figure 1, laminated glasses consist mostly of three layers. A local coordinate system is attached to each layer to allow for an efficient treatment of independent kinematics. In the following text, a quantity a expressed in a local coordinate system associated with the i-th layer is denoted as $a^{(i)}$, whereas a variable without an index represents a globally defined quantity, cf. Figure 1.

Each layer is modeled using the Timoshenko beam theory supplemented with membrane effects. Hence, the following kinematic assumptions are adopted

- the cross sections remain planar but not necessarily perpendicular to the deformed beam axis,
- vertical displacement does not vary along the height of the beam (when compared to the value of the displacement).

Non-zero displacement components in each layer are parametrized as:

$$\begin{aligned} u^{(i)}(x, z^{(i)}) &= u^{(i)}(x, 0) + \varphi^{(i)}(x) z^{(i)}, \\ w^{(i)}(x, z^{(i)}) &= w(x), \end{aligned}$$

where $i = 1, 2, 3$ and $z^{(i)}$ is measured in the local coordinate system from the middle plane of the i-th layer. The inter-layer interaction is ensured via the continuity conditions specified on

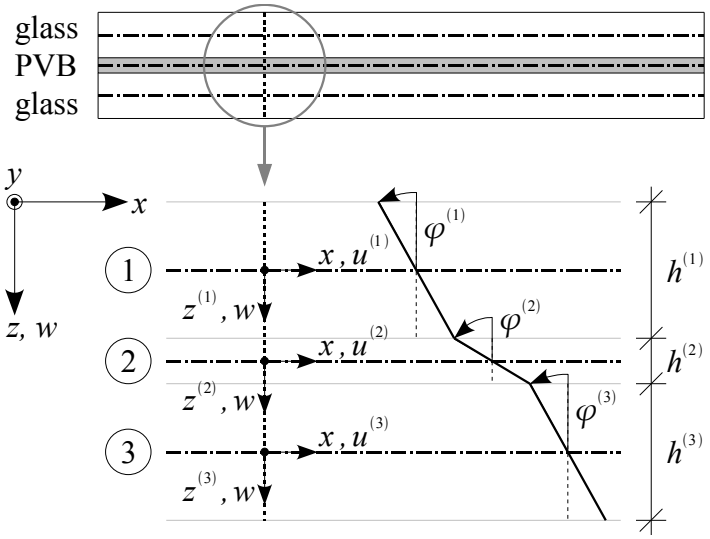

Figure 1: Kinematics of laminated beam

interfaces between layers in the form ($i = 1, 2$)

$$u^{(i)}(x, \frac{h^{(i)}}{2}) - u^{(i+1)}(x, -\frac{h^{(i+1)}}{2}) = 0. \tag{1}$$

The strain field in the i-th layer follows from the strain-displacement relations

$$\begin{aligned} \varepsilon_x^{(i)}(x, z^{(i)}) &= \frac{\partial u^{(i)}}{\partial x}(x, z^{(i)}) = \frac{\mathrm{d}u^{(i)}}{\mathrm{d}x}(x, 0) + \frac{\mathrm{d}\varphi^{(i)}}{\mathrm{d}x}(x) z^{(i)}, \\ \gamma_{xz}^{(i)}(x) &= \frac{\partial u^{(i)}}{\partial z^{(i)}}(x, z^{(i)}) + \frac{\partial w}{\partial x}(x) = \varphi^{(i)}(x) + \frac{\mathrm{d}w}{\mathrm{d}x}(x), \end{aligned}$$

which, when combined with the constitutive equations of each layer expressed in terms of the Young's modulus G and the shear moduli G

$$\sigma_x^{(i)}(x, z^{(i)}) = E^{(i)} \varepsilon_x^{(i)}(x, z^{(i)}) \quad \text{and} \quad \tau_{xz}^{(i)}(x) = G^{(i)} \gamma_{xz}^{(i)}(x),$$

yield the expression of the internal forces

$$\begin{aligned} N_x^{(i)}(x) &= E^{(i)} A^{(i)} \frac{\mathrm{d}u^{(i)}}{\mathrm{d}x}(x, 0), A^{(i)} = b h^{(i)}, \\ V_z^{(i)}(x) &= k G^{(i)} A^{(i)} \left(\varphi^{(i)}(x) + \frac{\mathrm{d}w}{\mathrm{d}x}(x) \right), k = \frac{5}{6}, \\ M_y^{(i)}(x) &= E^{(i)} I^{(i)} \frac{\mathrm{d}\varphi^{(i)}}{\mathrm{d}x}(x), I^{(i)} = \frac{1}{12} b (h^{(i)})^3, \end{aligned}$$

where b and $h^{(i)}$ are the width and height of the beam, recall Figure 1, and k, $A^{(i)}$ a $I^{(i)}$ stand for the shear correction factor, the cross-section area and the moment of inertia of the i-th layer, respectively.

To proceed, consider the weak form of the equilibrium equations, written for the i-th layer:[1]

$$\int_0^L \frac{\mathrm{d}}{\mathrm{d}x}\left(\delta u^{(i)}(x)\right) E^{(i)}A^{(i)}\frac{\mathrm{d}}{\mathrm{d}x}\left(u^{(i)}(x)\right)\,\mathrm{d}x = \int_0^L \delta u^{(i)}(x)\bar{f}_x^{(i)}(x)\,\mathrm{d}x + \left[\delta u(x)\bar{N}^{(i)}(x)\right]_0^L,$$

$$\int_0^L \frac{\mathrm{d}}{\mathrm{d}x}\left(\delta w(x)\right) kG^{(i)}A^{(i)}\gamma^{(i)}(x)\,\mathrm{d}x = \int_0^L \delta w(x)\bar{f}_z^{(i)}(x)\,\mathrm{d}x + \left[\delta w(x)\bar{Q}^{(i)}(x)\right]_0^L,$$

$$\int_0^L \frac{\mathrm{d}}{\mathrm{d}x}\left(\delta\varphi^{(i)}(x)\right) E^{(i)}I^{(i)}\frac{\mathrm{d}}{\mathrm{d}x}\left(\varphi^{(i)}(x)\right)\,\mathrm{d}x = \left[\delta\varphi^{(i)}(x)\bar{M}^{(i)}(x)\right]_0^L,$$

$$\int_0^L \delta\gamma^{(i)}(x)kG^{(i)}A^{(i)}\left[\gamma^{(i)}(x) - \varphi^{(i)}(x) - \frac{\mathrm{d}}{\mathrm{d}x}\left(w(x)\right)\right]\,\mathrm{d}x = 0.$$

to be satisfied for arbitrary admissible test fields $\delta u^{(i)}$, $\delta\varphi^{(i)}$ and δw. Note that the continuity conditions (1) will be introduced directly in the numerical formulation, as explained in the next Section.

4 Finite element discretization

To keep the discretization procedure transparent, it is assumed that each layer of the laminated beam is divided into identical number of elements, leading to the discretization scheme illustrated by Figure 2.

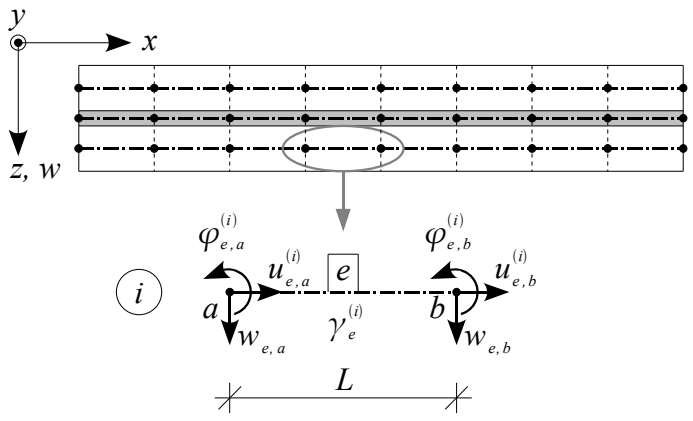

Figure 2: Finite element discretization of the i-th layer

Following the standard conforming Finite Element machinery, e.g. (Bathe, 1996), we ex-

[1] In order to simplify the notation, the subscripts $_x$ and $_z$ related to internal forces and kinematics-related quantities are omitted in the sequel.

press the searched and test displacement fields at the element level in the form

$$
\begin{aligned}
u_e^{(i)}(x) &\approx \mathsf{N}_{e,u}^{(i)}(x)\mathsf{r}_{e,u}^{(i)}, \qquad & \delta u_e^{(i)}(x) &\approx \mathsf{N}_{e,u}^{(i)}(x)\delta\mathsf{r}_{e,u}^{(i)},\\
w_e(x) &\approx \mathsf{N}_{e,w}(x)\mathsf{r}_{e,w}, & \delta w_e(x) &\approx \mathsf{N}_{e,w}(x)\delta\mathsf{r}_{e,w},\\
\varphi_e^{(i)}(x) &\approx \mathsf{N}_{e,\varphi}^{(i)}(x)\mathsf{r}_{e,\varphi}^{(i)}, & \delta\varphi_e^{(i)}(x) &\approx \mathsf{N}_{e,\varphi}^{(i)}(x)\delta\mathsf{r}_{e,\varphi}^{(i)},\\
\gamma_e^{(i)}(x) &\approx \mathsf{N}_{e,\gamma}^{(i)}(x)\mathsf{r}_{e,\gamma}^{(i)}, & \delta\gamma_e^{(i)}(x) &\approx \mathsf{N}_{e,\gamma}^{(i)}(x)\delta\mathsf{r}_{e,\gamma}^{(i)},
\end{aligned}
$$

where e is used to denote the element number, $\bullet_e$ and $\delta\bullet_e$ denote a relevant searched and test field restricted to the e-th element, $\mathsf{N}_{e,\bullet}^{(i)}$ is the associated matrix of basis functions and $\mathsf{r}_{e,\bullet}^{(i)}$ the matrix of nodal unknowns. In the actual implementation, the fields $u^{(i)}$, w_e and $\varphi_e^{(i)}$, as well as the corresponding test quantities, are assumed to be piecewise linear. To obtain a locking-free element, the shear strain $\gamma_e^{(i)}$ is assumed to be constant and is eliminated using the static condensation.

To simplify the further treatment, we consider the following partitioning of the stiffness matrix K and the right hand side matrix R related to the e-th element and the i-th layer:

$$
\begin{bmatrix} \mathsf{K}_e^{(i)} & \mathsf{K}_{ew}^{(i)} \\ \mathsf{K}_{we}^{(i)} & \mathsf{K}_w^{(i)} \end{bmatrix} \begin{bmatrix} \mathsf{r}_e^{(i)} \\ \mathsf{r}_{e,w} \end{bmatrix} = \begin{bmatrix} \mathsf{R}_e^{(i)} \\ \mathsf{R}_{e,w}^{(i)} \end{bmatrix},
$$

where $\mathsf{K}_{ew}^{(i)} = \left(\mathsf{K}_{we}^{(i)}\right)^{\mathsf{T}}$ and

$$
\mathsf{r}_e^{(i)} = \left[u_{e,a}^{(i)}, u_{e,b}^{(i)}, \varphi_{e,a}^{(i)}, \varphi_{e,b}^{(i)}\right]^{\mathsf{T}}, \qquad \mathsf{r}_{e,w} = \left[w_{e,a}, w_{e,b}\right]^{\mathsf{T}}.
$$

Considering all three layers together gives the stiffness matrix

$$
\begin{bmatrix}
\mathsf{K}_e^{(1)} & 0 & 0 & \mathsf{K}_{ew}^{(1)} & & \\
0 & \mathsf{K}_e^{(2)} & 0 & \mathsf{K}_{ew}^{(2)} & & \mathsf{E}_e{}^{\mathsf{T}} \\
0 & 0 & \mathsf{K}_e^{(3)} & \mathsf{K}_{ew}^{(3)} & & \\
\mathsf{K}_{we}^{(1)} & \mathsf{K}_{we}^{(2)} & \mathsf{K}_{we}^{(3)} & \mathsf{K}_w^{(1)} + \mathsf{K}_w^{(2)} + \mathsf{K}_w^{(3)} & 0 & \\
& \mathsf{E}_e & & 0 & 0 &
\end{bmatrix}
\begin{bmatrix} \mathsf{r}_e^{(1)} \\ \mathsf{r}_e^{(2)} \\ \mathsf{r}_e^{(3)} \\ \mathsf{r}_{e,w} \\ \lambda_{(4\times1)} \end{bmatrix} =
\begin{bmatrix} \mathsf{R}_e^{(1)} \\ \mathsf{R}_e^{(2)} \\ \mathsf{R}_e^{(3)} \\ \mathsf{R}_{e,w}^{(1)} + \mathsf{R}_{e,w}^{(2)} + \mathsf{R}_{e,w}^{(3)} \\ 0 \end{bmatrix},
$$

where λ stores the nodal values of the Lagrange multipliers, associated with the compatibility constraint (1), and the matrix

$$
\mathsf{E}_e = \begin{bmatrix}
1 & 0 & \frac{h^{(1)}}{2} & 0 & -1 & 0 & \frac{h^{(2)}}{2} & 0 & 0 & 0 & 0 & 0 \\
0 & 1 & 0 & \frac{h^{(1)}}{2} & 0 & -1 & 0 & \frac{h^{(2)}}{2} & 0 & 0 & 0 & 0 \\
0 & 0 & 0 & 0 & 1 & 0 & \frac{h^{(2)}}{2} & 0 & -1 & 0 & \frac{h^{(3)}}{2} & 0 \\
0 & 0 & 0 & 0 & 0 & 1 & 0 & \frac{h^{(2)}}{2} & 0 & -1 & 0 & \frac{h^{(3)}}{2}
\end{bmatrix}
$$

implements the tying conditions.

5 Results and discussion

To verify and validate the performance of the present approach, the previously described FEM model was implemented into MATLAB® system and compared the results against predictions

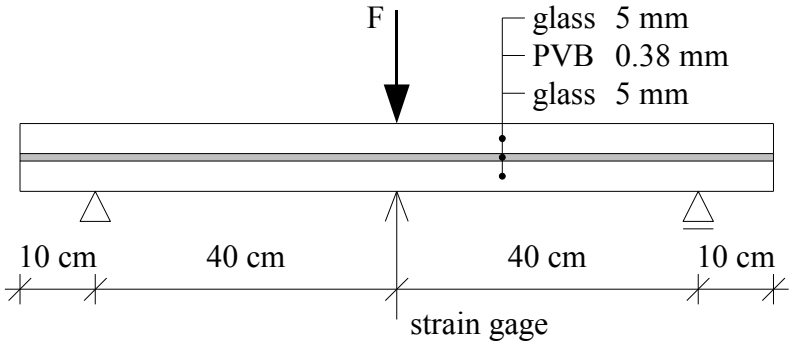

Figure 3: Three point bending setup for simply supported beam

Table 1: Material data

Glass	
Young's modulus, E	64.5 GPa
Poisson's ratio, ν	0.23
PVB layer	
Young's modulus, E	64.5 GPa
Poisson's ratio, ν	0.23

of an analytical model and experimental data for a three-point bending test on a simply supported laminated glass beam presented in (Asik and Tezcan, 2005) and schematically shown in Figure 3. The width of the beam is $b = 0.1$ m and material data of individual components of the layered beam are available in Table 1.

Table 2 summarizes values of the mid-span deflection for a representative load level determined by both models and the corresponding experimental values. In addition to the results obtained by an analytical method proposed by Asik and Tezcan (2005), results of the analysis by ADINA® system and the lower and upper bounds determined by the methods discussed in Section 1 are included. Clearly, the results of the last three method differ substantially from experimental data as well as the analytical results.

The proposed numerical model, on the other hand, show a response almost identical to the analytical method, which deviate from experimental measurement by less then 6%. Such accuracy can be considered as sufficient from the practical point of view.

Table 2: Comparison of results for a simply supported beam (load 50 N)

Model	Central deflection [mm]	η_{exp}	η_{an}
Laminated glass beam: thickness [mm] 5/0.38/5 (glass/PVB/glass)			
Experiment	1.27	-	-5.2%
Analytical model	1.34	5.5%	-
Numerical model	**1.34**	**5.5%**	**0.0%**
ADINA (Multilayered shell)	0.89	-30.2%	-33.8%
Monolithic glass beam: thickness [mm] 10 (glass+glass)			
Numerical model	0.99	-21.8%	-25.9%
Two independent glass beams: thickness [mm] 5/5 (without any interlayer)			
Numerical model	3.97	212.6%	196.2%

To further confirm predictive capacities of the proposed numerical scheme, a response corresponding to an increasing load is investigated in Tables 3 and 4. Again, the method seems to be sufficiently accurate in the investigated range of loads when considering the values of deflections as well as values of local stresses and strains.

Table 3: Comparison of deflections for a simply supported beam

Load [N]	Central deflection [mm]					
	w_{exp}	w_{an}	η_{exp}^{an} [%]	w_{num}	η_{exp}^{num} [%]	η_{an}^{num} [%]
50	1.27	1.34	5.51	1.34	5.51	0.00
100	2.55	2.69	5.49	2.68	5.10	-0.37
150	4.12	4.03	-2.18	4.02	-2.43	-0.25
200	5.57	5.38	-3.41	5.36	-3.77	-0.37

Table 4: Comparison of stresses and strains for a simply supported beam

Load [N]	Maximum strain [$\times 10^{-6}$]			Maximum stress [MPa]		
	ϵ_{an}	ϵ_{num}	η_{an}^{num} [%]	σ_{an}	σ_{num}	η_{an}^{num} [%]
50	112	114	1.79	7.23	7.34	1.52
100	224	228	1.79	14.45	14.68	1.59
150	336	341	1.49	21.68	22.02	1.57
200	448	455	1.56	28.9	29.36	1.59

6 Conclusions

As shown by the presented results, the proposed numerical method is well-suited for the modeling of laminated beams, mainly because of its low computational cost and accurate representation of the structural member behavior. Future improvements of the model will consider large deflections and the time-dependent response of the interlayer and will be reported separately.

Acknowledgments

The support provided by the GAČR grant No. 106/07/1244 is gratefully acknowledged.

References

Asik, M. Z. (2003). Laminated glass plates: Revealing of nonlinear behavior. *Computers and Structures*, 81:2659–2671.

Asik, M. Z. and Tezcan, S. (2005). A mathematical model for the behavior of laminated glass beams. *Computers and Structures*, 83:1742–1753.

Bathe, K. J. (1996). *Finite Element Procedures*. Prentice Hall, second edition.

Duser, A. V., Jagota, A., and Bennison, S. J. (1999). Analysis of glass/polyvinyl butyral laminates subjected to uniform pressure. *Journal of Engineering Mechanics*, 125:435–442.

Ivanov, I. V. (2006). Analysis, modelling, and optimization of laminated glasses as plane beam. *International Journal of Solids and Structures*, 43:6887–6907.

Matouš, K., Šejnoha, M., and Šejnoha, J. (1998). Energy based optimization of layered beam structures. *Acta Polytechnica*, 38(2):5–15.

Mau, S. T. (1973). A refined laminated plate theory. *Journal of Applied Mechanics–Transactions of the ASME*, 40(2):606–607.

Norville, H. S., King, K. W., and Swofford, J. L. (1998). Behavior and strength of laminated glass. *Journal of Engineering Mechanics*, 124:46–53.

Vallabhan, C. V. G., Das, Y. C., Magdi, M., Asik, M., and Bailey, J. R. (1993). Analysis of laminated glass units. *Journal of Structural Engineering*, 113:1572–1585.

Vallabhan, C. V. G., Minor, J. E., and Nagalla, S. R. (1987). Stress in layered glass units and monolithic glass plates. *Journal of Structural Engineering*, 113:36–43.

Šejnoha, M. (1996). *Micromechanical Modeling of Unidirectional Fibrous Composite Plies and Laminates*. PhD thesis, Rensselaer Polytechnic Institute, Troy, NY.